

Magnetic properties of antiferromagnetic $\text{Ni}_{1-x}\text{Zn}_x\text{F}_2$ and $\text{Ni}_{1-x}\text{Mg}_x\text{F}_2$

A. N. Bazhan, V. N. Bevz, and S. V. Petrov

Institute for Physical Problems, Academy of Sciences of the USSR

(Submitted 12 June 1987)

Zh. Eksp. Teor. Fiz. 94, 231–243 (April 1988)

The magnetic properties are investigated for $\text{Ni}_{1-x}\text{Zn}_x\text{F}_2$ and $\text{Ni}_{1-x}\text{Mg}_x\text{F}_2$ single crystals (with $x < x_c = 0.75$, the percolation limit), for which the interacting magnetic ions (Ni^{++}) are randomly distributed in the crystal lattice. An antiferromagnetic state with a weak ferromagnetic moment is present in the single crystals at temperatures $T < T_N(x)$. The strength $H_D = \sigma_D/\chi_1$ of the Dzyaloshinskii interaction responsible for the weak ferromagnetic moment is essentially independent of the concentration of the nonmagnetic ions, $H_D = 27.2 \pm 0.5$ kOe. The dependence $M(H, T)$ is found to become nonlinear with decreasing temperature when \mathbf{H} is normal to the tetragonal axis; in addition, the weak ferromagnetic moment is found to depend linearly on temperature, $\sigma_D(T) \propto (1 - \eta T/T_N)$, for $T < T_N$. This behavior is most pronounced as x approaches the percolation limit x_c .

The magnetic properties of $\text{Mn}_{1-x}\text{Zn}_x\text{F}_2$, $\text{Co}_{1-x}\text{Zn}_x\text{F}_2$, and $\text{Fe}_{1-x}\text{Zn}_x\text{F}_2$ single crystals, in which the interacting magnetic ions are randomly distributed in a tetragonal crystal lattice, are currently under active study.^{1–5} For Zn^{++} ion concentrations below the percolation limit $x_c = 0.75$, all these materials become antiferromagnetic upon cooling, and the antiferromagnetic vector \mathbf{L} points preferentially along the tetragonal axis. The unique magnetic properties of these materials are a consequence of the random internal distribution of the exchange and anisotropic interactions and may be attributed to the formation of magnetic clusters as x increases above 0.25 and T decreases. The correlation radius of this new magnetic state is finite,^{1–4} and the antiferromagnetic vector is essentially parallel to the tetragonal axis, deviating from it randomly by a small angle.

It is found that NiF_2 single crystals become antiferromagnetic at $T_N = 73$ K (Ref. 6). Unlike MnF_2 , CoF_2 , and FeF_2 , the antiferromagnetic vector \mathbf{L} in NiF_2 points along the binary axes [100] or [010], and the crystal becomes weakly ferromagnetic because of the Dzyaloshinskii-Mori interaction, which is determined by the single-ion anisotropy in crystals with tetragonal symmetry.

The purpose of the present work is to study the magnetic properties of dilute antiferromagnets of composition $\text{Ni}_{1-x}(\text{Zn, Mg})_x\text{F}_2$ with $x < x_c$, which when cooled also undergo a transition to an antiferromagnetic state with a weak ferromagnetic moment σ_D (Ref. 5).

If the interacting ions are randomly distributed in the $\text{Ni}_{1-x}(\text{Zn, Mg})_x\text{F}_2$, then the same is true of the exchange and anisotropic relativistic interactions, and in particular the Dzyaloshinskii interaction. Because the latter interaction, which is responsible for the weak ferromagnetism in NiF_2 , stems from the single-ion anisotropy of the Ni^{++} ions in the crystal lattice, it should not depend on their concentration, apart from the small x -dependence of the lattice constants for NiF_2 , ZnF_2 , MgF_2 , and $\text{Ni}_{1-x}(\text{Zn, Mg})_x\text{F}_2$. One anticipates that as the Zn^{++} or Mg^{++} concentration increases and the exchange and anisotropic dipole interactions become weaker, the Dzyaloshinskii interaction should play a more important role in determining the magnetic properties.

It should be noted that just as for MnF_2 , the exchange interaction measured⁷ along the [100] or [010] binary axes

for Ni^{++} ions belonging to a single magnetic sublattice in NiF_2 is found to be negative. This suggests that as the Zn^{++} or Mg^{++} ion concentration increases, the effective “ \pm ”-exchange interactions of the Ni^{++} ions should become randomly distributed along the [100] and [010] axes in dilute antiferromagnetic $\text{Ni}_{1-x}(\text{Zn, Mg})_x\text{F}_2$. Such a distribution may alter the magnetic properties of the $\text{Ni}_{1-x}(\text{Zn, Mg})_x\text{F}_2$ due to possible competition between the magnetic structures.

We investigated the magnetic properties of $\text{Ni}_{1-x}(\text{Zn, Mg})_x\text{F}_2$ single crystals by using a vibrating magnetometer, which enabled us to measure all three mutually perpendicular components of the magnetic moment of the specimen.⁸ We studied how the magnetic moments of the single crystals depended on the applied magnetic field for various field orientations and temperatures.

The experiments were performed on several $\text{Ni}_{1-x}\text{Zn}_x\text{F}_2$ and $\text{Ni}_{1-x}\text{Mg}_x\text{F}_2$ single crystals, $x = 0.3$ –0.6, grown here at the Institute for Physical Problems (in this paper we use $\text{Ni}_{1-x}(\text{Zn, Mg})_x\text{F}_2$ to denote the crystals). The concentration of the magnetic ions (Ni^{++}) in $\text{Ni}_{1-x}(\text{Zn, Mg})_x\text{F}_2$ was deduced from the temperature dependence of the magnetic susceptibility in the paramagnetic state ($T \gg T_N$):

$$\chi(T) = N(x)(\mu_B)^2 S(S+1)/3k[T + \Theta(x)].$$

The large error ~ 10 –15% in finding the Ni^{++} concentration was due to the small size of the crystals (diameter ~ 0.5 mm, mass ~ 1 mg).

EXPERIMENTAL RESULTS

Figure 1a–e shows how the magnetic moments for NiF_2 and $\text{Ni}_{1-x}(\text{Zn, Mg})_x\text{F}_2$ single crystals depend on the applied magnetic field H directed along the C_2 binary axis at several temperatures. The experimental data shown in Fig. 1 demonstrate that just as in the case of NiF_2 for temperatures $T < T_N = 73$ K, the $\text{Ni}_{1-x}(\text{Zn, Mg})_x\text{F}_2$ single crystals undergo a transition to an antiferromagnetic state with a weak ferromagnetic moment when $T < T_N(x)$. The dependence $M(H, T)$ for $\text{Ni}_{1-x}(\text{Zn, Mg})_x\text{F}_2$ with $x < 0.75$ is described by $M(H, T) = \sigma_D(T) + \chi_1 H$ for $T < T_N(x)$ and $\mathbf{H} \parallel [100]$. We see that for $T < T_N$, $M(H, T)$ for the $\text{Ni}_{1-x}(\text{Zn, Mg})_x\text{F}_2$ single crystals becomes nonlinear in strong magnet-

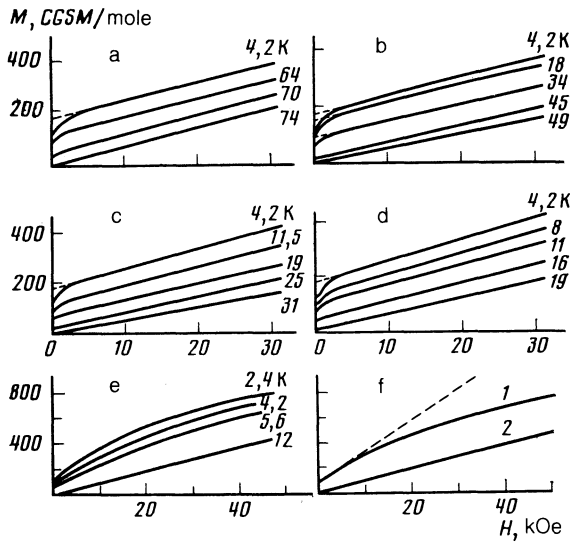


FIG. 1. Magnetic moments of $\text{Ni}_{1-x}(\text{Zn}, \text{Mg})_x\text{F}_2$ single crystals as functions of the applied magnetic field $\mathbf{H} \parallel [100]$ for several temperatures and nonmagnetic ion concentrations: a) $x = 0$; b) 0.3; c) 0.55; d) 0.63; e) 0.72; f) curves 1 and 2 give $M(H)$ at $T = 4.2$ K for $x = 0.72$, with \mathbf{H} along the [100] and [001] axes, respectively.

ic fields $H > 30$ kOe, and the magnetic susceptibility χ_\perp^* measured in weak magnetic fields < 20 kOe is temperature-dependent, as can be seen from the change in the slope of the curves $M(H, T)$ in Fig. 1. This behavior is most pronounced for large nonmagnetic ion concentrations $x = 0.63, x = 0.72$ (Fig. 1d, e). As the Zn^{++} or Mg^{++} ion concentration increases in the $\text{Ni}_{1-x}(\text{Zn}, \text{Mg})_x\text{F}_2$ single crystals and approaches x_c , the nonlinear dependence $M(H, T)$, arising in the plane normal to the tetragonal axis, is observed throughout the range of magnetic fields employed. Figure 1e shows $M(H, T)$ for $\text{Ni}_{0.28}\text{Mg}_{0.72}\text{F}_2$, $T_N = 8 \pm 0.5$ K. It is clear from the figure that for this crystal, $M(H, T)$ is nonlinear even in the weakest magnetic fields. Figure 1f shows $M(H)$ for $\text{Ni}_{0.28}\text{Mg}_{0.72}\text{F}_2$ at $T = 4.2$ K with the applied magnetic field \mathbf{H} along the binary [100] (1) and tetragonal [001] axes (2), respectively. We see that for $\text{Ni}_{0.28}\text{Mg}_{0.72}\text{F}_2$, $M(H)$ becomes nonlinear at weak fields only when $\mathbf{H} \parallel [100]$. The dependence is observed to be linear: $M(H) = \chi_\perp H$ for \mathbf{H} along the tetragonal axis.

Analysis of the experimental curves $M(H, T)$ for all the $\text{Ni}_{1-x}(\text{Zn}, \text{Mg})_x\text{F}_2$ single crystals, various magnetic field orientations, and $T \ll T_N(x)$ revealed that $M(H, T) = \chi_\perp H$ for \mathbf{H} parallel to the tetragonal [001] axis, while for \mathbf{H} along the [110] binary axis we have $M(H) = \sigma_D^{**} + \chi^{**}H$ in weak magnetic fields; here $\sigma_D^{**} = 2^{-1/2}\sigma_D$ and $\chi \approx (1/2)\cdot\chi_\perp$. We conclude from an analysis of $M(H)$ for these two orientations of \mathbf{H} that just as for antiferromagnetic NiF_2 , for $T \ll T_N(x)$ the antiferromagnetic vector $\langle \mathbf{L} \rangle$ in antiferromagnetic $\text{Ni}_{1-x}(\text{Zn}, \text{Mg})_x\text{F}_2$ is parallel to the [100] or [010] binary axes and perpendicular to the tetragonal axis. (We note that in these crystals \mathbf{L} may be defined as $\langle \mathbf{L} \rangle = \langle \mathbf{M}_1 \rangle - \langle \mathbf{M}_2 \rangle$, where $\langle \mathbf{M}_i \rangle$ is the average magnetic moment of the i th sublattice.) The ferromagnetic moment is normal to $\langle \mathbf{L} \rangle$. The curve $M(H)$ for $\text{Ni}_{0.28}\text{Mg}_{0.72}\text{F}_2$ single crystals with $x \approx x_c$ and $\mathbf{H} \parallel [100]$ differs greatly from $M(H)$ for the NiF_2 single crystals. This may reflect the random distribution of the interacting magnetic ions and hence of the

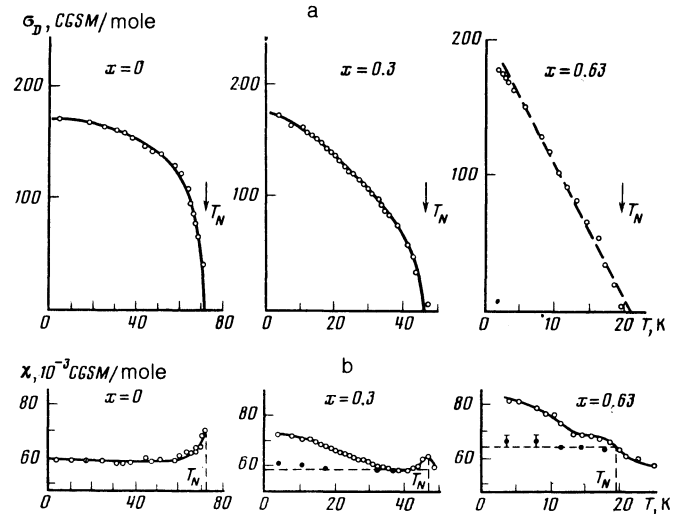


FIG. 2. a) Temperature dependence of the weak ferromagnetic moment for $\text{Ni}_{1-x}(\text{Zn}, \text{Mg})_x\text{F}_2$ single crystals; b) temperature dependence of the magnetic susceptibilities for $\text{Ni}_{1-x}(\text{Zn}, \text{Mg})_x\text{F}_2$ single crystals measured in weak (\circ) and strong (\bullet) magnetic fields (< 20 kOe and > 30 kOe, respectively).

Dzyaloshinskii interaction acting in the (001) plane of the crystal.

Figure 2a shows the temperature dependence of the weak ferromagnetic moment in the NiF_2 and $\text{Ni}_{1-x}(\text{Zn}, \text{Mg})_x\text{F}_2$ single crystals. These results were obtained by extrapolating the curves $M(H, T)$ to zero magnetic field. As x increases, the ferromagnetic moments σ_D for $\text{Ni}_{1-x}(\text{Zn}, \text{Mg})_x\text{F}_2$ become larger than for NiF_2 , although the increase is less than the experimental error. For NiF_2 single crystals, $\sigma_D(0) = 169 \pm 10$ CGSM/mole.

Figure 2b shows the temperature dependence of the magnetic susceptibilities χ_\perp^* and χ_\perp measured in relatively weak (< 20 kOe) and strong fields (> 30 kOe). We see from Fig. 2a that as x increases, $\sigma_D(T)$ for $\text{Ni}_{1-x}(\text{Zn}, \text{Mg})_x\text{F}_2$ differs greatly from $\sigma_D(T)$ for NiF_2 single crystals. Figure 3 compares $\sigma_D(T)$ for several $\text{Ni}_{1-x}(\text{Zn}, \text{Mg})_x\text{F}_2$ single crystals; $\sigma_D(T)/\sigma_D(0)$ is plotted as a function of T/T_N . We see that as x increases, $\sigma_D(T)$ departs increasingly from the

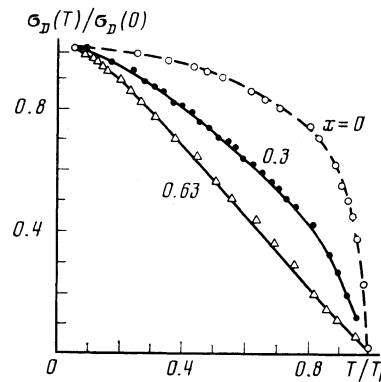


FIG. 3. Reduced ferromagnetic moments $\sigma_D(T)/\sigma_D(0)$ for $\text{Ni}_{1-x}(\text{Zn}, \text{Mg})_x\text{F}_2$ single crystals ($x = 0, 0.3, 0.63$) as a function of the reduced temperature T/T_N .

corresponding curve for NiF_2 . For $\text{Ni}_{0.37}\text{Mg}_{0.63}\text{F}_2$ ($T_N = 19.0 \pm 0.5$ K) and $3.5 < T < 18$ K, $\sigma_D(T)$ can be approximated by $\sigma_D(T) = \sigma_D^*(0)(1 - \eta T/T_N)$. For $T < 3.4$ K or $18 < T < T_N$, the experimental $\sigma_D(T)$ curve departs slightly from the linear dependence observed for $3.5 < T < 18$ K. A linear $\sigma_D(T)$ dependence for $2 < T < T_N$ is also observed for $\text{Ni}_{0.28}\text{Mg}_{0.72}\text{F}_2$, for which the Néel temperature is $T_N = 8 \pm 0.5$ K.

It is clear from the results in Fig. 2b that the strong-field magnetic susceptibility of the $\text{Ni}_{1-x}(\text{Zn}, \text{Mg})_x\text{F}_2$ single crystals is independent of temperature. It is natural to identify this magnetic susceptibility with the "perpendicular" magnetic susceptibility of the crystals. As in the case of NiF_2 single crystals, at $T \approx T_N$ the magnetic susceptibility of the $\text{Ni}_{1-x}(\text{Zn}, \text{Mg})_x\text{F}_2$ crystals increases. This corresponds to the onset of a field-induced antiferromagnetic ordering at $T = T_N$ in weakly ferromagnetic single crystals.⁹ It is clear from Fig. 2b that the magnetic susceptibility for $\text{Ni}_{1-x}(\text{Zn}, \text{Mg})_x\text{F}_2$ measured in weak fields $H < 20$ kOe increases with decreasing temperature $T \ll T_N(x)$. This increase in $\chi_1^*(T)$ as $T \rightarrow 0$ is analogous to that observed in Ref. 10 for $\text{Mn}_{1-x}\text{Zn}_x\text{F}_2$ single crystals cooled in weak magnetic fields. However, the field interval $H < 20$ kOe within which $\chi_1^*(T)$ for $\text{Ni}_{1-x}(\text{Zn}, \text{Mg})_x\text{F}_2$ increases with $1/T$ is considerably larger than for $\text{Mn}_{1-x}\text{Zn}_x\text{F}_2$. The behavior of $\chi_1^*(T)$ as $H \rightarrow 0$ was determined for $\text{Mn}_{1-x}\text{Zn}_x\text{F}_2$ single crystals in Ref. 10; however this is difficult to do for $\text{Ni}_{1-x}(\text{Zn}, \text{Mg})_x\text{F}_2$, because the weak ferromagnetic moment $\sigma_D(H, T)$ changes sign in magnetic fields $H \rightarrow 0$. The increasing dependences $\chi_1^*(T)$ for $\text{Ni}_{1-x}(\text{Zn}, \text{Mg})_x\text{F}_2$ and $\text{Mn}_{1-x}\text{Zn}_x\text{F}_2$ single crystals¹⁰ differ because in the present work they were obtained at higher magnetic fields $H > 5$ kOe. Thus unlike the situation for NiF_2 crystals, χ_1^* for $\text{Ni}_{1-x}(\text{Zn}, \text{Mg})_x\text{F}_2$ single crystals increases with decreasing temperature $T < T_N$ when $H < 20$ kOe, while for strong magnetic fields $H > 30$ kOe χ_1 is independent of T .

Figure 4 shows how the antiferromagnetic transition temperature $T_N(x)$, ferromagnetic moment $\sigma_D(x)$, and strong-field magnetic susceptibility depend on the Zn^{++} , Mg^{++} ion concentration for the $\text{Ni}_{1-x}(\text{Zn}, \text{Mg})_x\text{F}_2$ single

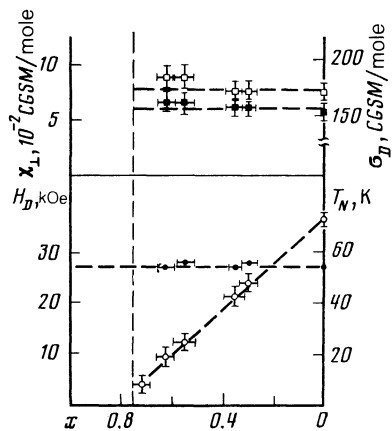


FIG. 4. Antiferromagnetic transition temperature T_N (○), weak ferromagnetic moment σ_D (□), magnetic susceptibility χ_1 (■), and effective Dzyaloshinskii field $H_D = \sigma_D/\chi_1$ (●) as functions of the concentration of the nonmagnetic ions Zn^{++} , Mg^{++} for $\text{Ni}_{1-x}(\text{Zn}, \text{Mg})_x\text{F}_2$ single crystals (percolation limit $x_c = 0.75 \pm 0.02$).

crystals that we investigated. The effective Dzyaloshinskii field $H_D = \sigma_D/\chi_1$ responsible for the weak ferromagnetism in $\text{Ni}_{1-x}(\text{Zn}, \text{Mg})_x\text{F}_2$ is also shown in Fig. 4 as a function of the concentration of the nonmagnetic ions. The value of σ_D used to calculate H_D was found by extrapolating the curves $M(H)$ for weak magnetic fields to $H = 0$ and extrapolating $\sigma_D(T)$ to $T = 0$. The susceptibility χ_1 used in calculating H_D was found from the temperature-independent slope of the curve $M(H)$ in strong magnetic fields, or else was taken equal to the magnetic susceptibility χ_1 of $\text{Ni}_{1-x}(\text{Zn}, \text{Mg})_x\text{F}_2$ near the Néel temperature T_N . For $\text{Ni}_{0.28}\text{Mg}_{0.72}\text{F}_2$ it was more difficult to find σ_D , χ_1 , and H_D because the dependence $M(H, T)$ was nonlinear for all magnetic fields with \mathbf{H} in the (001) plane.

The phase transition temperature $T_N(x)$ was determined from the maximum susceptibility $\chi_1(T_N)$ and from the condition that the weak ferromagnetism $\sigma_D(T_N)$ vanishes. We see from Fig. 4 that although T_N for antiferromagnetic $\text{Ni}_{1-x}\text{Mg}_x\text{F}_2$ decreases considerably as x increases (from $T_N = 73$ K for NiF_2 to $T_N = 8 \pm 0.5$ K for $\text{Ni}_{0.28}\text{Mg}_{0.72}\text{F}_2$), σ_D and χ_1 are independent of x to within 10%. The effective Dzyaloshinskii field $H_D = 27.2 \pm 0.5$ K is also essentially independent of x . Again, it is difficult to determine H_D for $x = 0.28$ owing to the strong nonlinearity of $M(H)$.

Figure 4 shows that for Zn^{++} or Mg^{++} ion concentrations $x_c = 0.75-0.8$, above the percolation limit, there is no antiferromagnetic ordering in the $\text{Ni}_{1-x}(\text{Zn}, \text{Mg})_x\text{F}_2$ single crystals. Our preliminary data on the magnetic properties for $\text{Ni}_{0.2}\text{Mg}_{0.8}\text{F}_2$ single crystals indicate that no antiferromagnetic phase with a weak ferromagnetic moment is present.

Figure 5 shows the magnetic moment for an $\text{Ni}_{0.45}\text{Mg}_{0.55}\text{F}_2$ single crystal at several temperatures as a function of the applied magnetic field for \mathbf{H} along the [100] and [110] axes. We see from the experimental results shown in the figure that for this crystal, just as for NiF_2 (Ref. 6), $M(H, T)$ depends on the field orientation when $T \ll T_N$, and in fact (as pointed out above)

$$\sigma_D(\mathbf{H} \parallel [110]) = 2^{-\nu} \sigma_D(\mathbf{H} \parallel [100]).$$

This relation supports the conclusion that the ferromagnetic moment σ_D in $\text{Ni}_{1-x}(\text{Zn}, \text{Mg})_x\text{F}_2$ single crystals is direct-

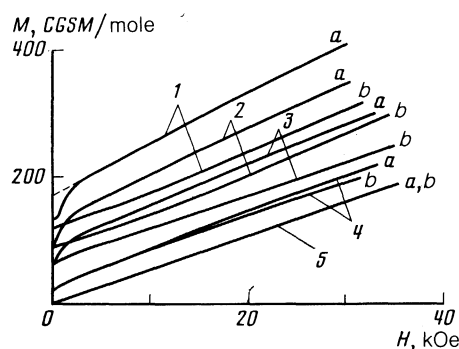


FIG. 5. Magnetic moments for an $\text{Ni}_{0.45}\text{Mg}_{0.55}\text{F}_2$ single crystal versus applied magnetic field for $\mathbf{H} \parallel [100]$ (curves a) and $\mathbf{H} \parallel [110]$ (curves b) for: 1) $T = 4.2$; 2) 11.2; 3) 18; 4) 24.5; 5) 45 K.

ed along the [100] or [010] binary axes. For \mathbf{H} increasing along the [110] axis, $M(H)$ for $x = 0.55$ becomes nonlinear in the same way as $M(H)$ for NiF_2 with $\mathbf{H} \parallel [110]$ (Ref. 6). Moreover, $M(H)$ becomes linear $M(H) = \chi_1 H$, in the strong-field limit. This indicates that as $\mathbf{H} \parallel [110]$ increases, the antiferromagnetic vector \mathbf{L} rotates away from the [100] axis toward the [110] axis normal to the applied field \mathbf{H} , and the weak ferromagnetic moment σ_D disappears.⁶

We also see from Fig. 5 that the curves $M(H, T)$ for $\mathbf{H} \parallel [100]$ and $\mathbf{H} \parallel [110]$ coalesce as T increases to T_N , and we have $M(H, T) = \sigma_D(T) + \chi_1 H$ for all field strengths and orientations in the (001) plane. This anisotropy of the magnetic properties of $\text{Ni}_{1-x}(\text{Zn}, \text{Mg})_x\text{F}_2$ for $T \ll T_N(X)$ and its behavior as $T \rightarrow T_N(x)$ recall the situation observed for NiF_2 in Ref. 6. We note only that the additional nonlinearity in $M(H, T)$ at strong fields for $\text{Ni}_{1-x}(\text{Zn}, \text{Mg})_x\text{F}_2$ with $x \approx x_c$ makes it difficult to numerically analyze the data for $\mathbf{H} \parallel [110]$, as was done in Ref. 6 to study the rotation of \mathbf{L} in NiF_2 as $\mathbf{H} \parallel [110]$ increases.

DISCUSSION

As previously in the case of NiF_2 , we use the thermodynamic potential, derived by Dzyaloshinskii¹¹ from symmetry considerations for crystals with the D_{4h} tetragonal symmetry,¹⁴ to describe the magnetic properties of $\text{Ni}_{1-x}(\text{Zn}, \text{Mg})_x\text{F}_2$ single crystals as $T < T_N$ decreases. This potential is given by

$$\begin{aligned}\Phi = & \frac{1}{2}Bm^2 + \frac{1}{2}D(\gamma m)^2 + \frac{1}{2}a\gamma_z^2 + \frac{1}{2}bm_z^2 \\ & - e(\gamma_x m_y + \gamma_y m_x) + \frac{1}{2}bg\gamma_x^2 \gamma_y^2 - 2d(\gamma m)\gamma_x \gamma_y - m\mathbf{H}.\end{aligned}\quad (1)$$

In dilute antiferromagnetic $\text{Ni}_{1-x}(\text{Zn}, \text{Mg})_x\text{F}_2$ with $0 < x < x_c$, the vectors \mathbf{m} and γ during the transition to the antiferromagnetic state are expressible in terms of the magnetic moments of the Ni^{++} ion sublattices averaged over the unit cells: $m = \langle \mathbf{M}_1 \rangle + \langle \mathbf{M}_2 \rangle$ and $\gamma = (\langle \mathbf{M}_1 \rangle - \langle \mathbf{M}_2 \rangle)/2M_0$.

The invariants $\frac{1}{2} \cdot Bm^2$ and $\frac{1}{2} \cdot D(\gamma m)^2$ describe the exchange interaction of the Ni^{++} magnetic moments, and $H_E = M_0 B = M_0/\chi_1$, $H_E^* = M_0/\chi_{\parallel} = M_0/(B + D)$, where χ_1 and χ_{\parallel} are the transverse ($\mathbf{H} \perp \mathbf{L}$) and longitudinal ($\mathbf{H} \parallel \mathbf{L}$) magnetic susceptibilities. The invariant $e(\gamma_x m_y + \gamma_y m_x)$ appears because the antiferromagnetic state also possesses a weak transverse ferromagnetic moment $\sigma_D = e/B = \chi_1 H_{D1}$. The other invariants determine the direction of the antiferromagnetic vector \mathbf{L} in the crystal and the weak longitudinal ferromagnetic moment

$$\sigma_{D\parallel} = \chi_{\parallel} H_{D\parallel} = (e + d)/(B + D)$$

(with $\mathbf{L} \parallel [100]$) in the crystals. We conclude from the experimental results in Figs. 1 and 2 that in the antiferromagnetic state ($T \ll T_N(x)$, Fig. 4) the $\text{Ni}_{1-x}(\text{Zn}, \text{Mg})_x\text{F}_2$ sin-

gle crystals have a weak ferromagnetic moment σ_{D1} which is normal to the [001] tetragonal axis and parallel to the [100] or [010] binary axes.

We thus conclude that the antiferromagnetic properties and the weak ferromagnetism of the $\text{Ni}_{1-x}(\text{Zn}, \text{Mg})_x\text{F}_2$ specimens are describable using the thermodynamic potential (1), with \mathbf{m} and γ averaged over the unit cells. The effective Dzyaloshinskii interaction $H_D = \sigma_D/\chi_1$ responsible for the weak ferromagnetism is essentially independent of x . Since the transition temperature $T_N(x)$ to the antiferromagnetic phase decreases with Zn^{++} or Mg^{++} concentration, the same is true of the Ni^{++} exchange interaction. Allowing for the concentration of the magnetic ions, we conclude that the effective Dzyaloshinskii interaction (acting on a single Ni^{++} ion in the crystal) increases. Figure 6a-d schematically shows the average magnetic moment vectors in the NiF_2 and $\text{Ni}_{1-x}(\text{Zn}, \text{Mg})_x\text{F}_2$ crystals. As the magnetic ions are replaced by nonmagnetic ions, the angle between the magnetic moments of the sublattices increases, so that σ_D for any pair of antiferromagnetically coupled ions also increases. We see that σ_D , χ_1 , and H_D depend only weakly on the concentration of the magnetic ions Ni^{++} (see Fig. 4). This experimental result stems from the fact that the weak ferromagnetism in NiF_2 and $\text{Ni}_{1-x}(\text{Zn}, \text{Mg})_x\text{F}_2$ is a consequence of the single ion anisotropy, which for a given magnetic ion depends only on the position of the F^- ions and is independent of the number of magnetic neighbors. The invariant responsible for the weak ferromagnetic moment σ_D can be expressed as

$$e \sum_i (S_i^z S_i^y - S_i^x S_i^y). \quad (2)$$

The relation $H_D \approx H_e$ may become satisfied as the concentration of the nonmagnetic ions increases and the mean exchange interactions H_E in the $\text{Ni}_{1-x}(\text{Zn}, \text{Mg})_x\text{F}_2$ single crystals become weaker. The average magnetic moment of the Ni^{++} sublattices must lie along the [110] or [110] axes (Fig. 6a). In our experiments (see Fig. 1c) we conclude by comparing the phase transition temperature T_N for $\text{Ni}_{0.28}\text{Mg}_{0.72}\text{F}_2$ with T_N for NiF_2 that in this case $H_D/H_E \approx 0.3$. The mean angle between the Ni^{++} magnetic moments and the [100] or [010] binary axes in the (001) plane is approximately 20° . The interacting magnetic ions and the anisotropic interactions were thus randomly distributed in our crystals.

The random distribution of the interacting ions causes the Dzyaloshinskii interaction to be randomly distributed in the (001) plane, which is reflected in a random distribution of the alignments of the magnetic moments of the ions relative to the [100] or [010] axes in the (001) plane; this distribution is such that the mean orientation of the weak ferromagnetic moment is along the binary axes (see Fig. 6d). The experimental results in Fig. 1e show that for this orientation

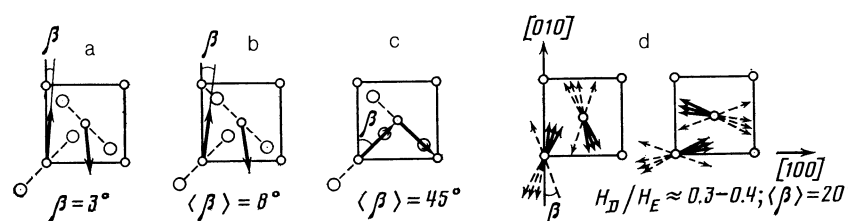


FIG. 6. Sketch showing the average orientations of the Ni^{++} magnetic moments in the $\text{Ni}_{1-x}(\text{Zn}, \text{Mg})_x\text{F}_2$ lattices. These results were obtained for increasing x ($x < x_c$) by comparing the mean effective exchange and Dzyaloshinskii interactions: a) $x = 0$, $H_D/H_E = 2.7 \cdot 10^{-2}$; b) $x = 0.55$, $\langle H_D \rangle / \langle H_E \rangle = 10^{-1}$; c) $\langle H_D \rangle / \langle H_E \rangle \approx 1$; d) $\langle H_D \rangle / \langle H_E \rangle = 0.3-0.4$ (the distribution of the Ni^{++} orientations is sketched for $\text{Ni}_{0.28}\text{Mg}_{0.72}\text{F}_2$).

of σ_D , the curve $M(H)$ is nonlinear when H is applied along the [100] or [010] binary axes, but linear ($M(H) = \chi_1 H$) when H is along the tetragonal axis. If for $H \parallel [100]$ we approximate the nonlinear dependence $M(H, T)$ in Fig. 1e by the expression

$$M(H, T) = \sigma_D(T) + \chi_1(T)H - \chi_s(T)H^\alpha,$$

where $\sigma_D(T)$ is the ferromagnetic moment and $\chi_1(T)H$ gives the linear weak-field dependence ($H < 2-3$ kOe, dashed line in Fig. 1e), we find that $\alpha = 1.66 \pm 0.3$, and the approximation is valid for fields < 50 kOe. For the magnetic fields used in our experiment, $M(H)$ is observed to be nonlinear for strong fields $H \parallel [001]$. It should also be noted that this nonlinear dependence $M(H)$ for $\text{Ni}_{0.28}\text{Mg}_{0.72}\text{F}_2$ can be approximated by $M(H, T) = \sigma_D(T) + \chi H^\gamma$ with $\gamma = 0.66 \pm 0.1$, for fields below 30 kOe. The nonlinearity of $M(H)$ for H in the (001) plane indicates that as T decreases, the (001) plane in $\text{Ni}_{1-x}\text{Mg}_x\text{F}_2$ single crystals with $x \rightarrow x_c$ enters a state in which the ion magnetic moments are randomly aligned, as in a spin glass. The effective Dzyaloshinskii interaction in the (001) plane is responsible for the random alignment of the Ni^{++} magnetic moments in $\text{Ni}_{0.28}\text{Mg}_{0.72}\text{F}_2$ in the plane normal to the tetragonal axis (Fig. 6d).

The values $H_E = 1000 \pm 100$, 670 ± 60 , and 220 ± 20 kOe were obtained for the exchange interaction for $\text{Ni}_{1-x}(\text{Zn, Mg})_x\text{F}_2$ crystals with $x = 0$, 0.7, and 0.37, respectively. To calculate H_E one must use the experimentally measured susceptibility for strong fields, since this magnetic susceptibility is temperature-independent.

A distinctive feature of these crystals is the temperature dependence of the magnetic susceptibility for weak fields < 20 kOe; for both $H \parallel C_4$ and $H \parallel C_4$, χ increases with increasing $x \rightarrow x_c = 0.75 \pm 0.05$. In addition, the temperature dependence $\sigma_{D\perp}(T)$ of the weak ferromagnetic moment becomes linear as the concentration of Zn^{++} or Mg^{++} ions increases.

For $T \ll T_N(x)$ we have $\sigma_D(T) = \sigma_D(0)(1 - \beta T^2)$ for NiF_2 single crystals. As the $(\text{Zn, Mg})^{++}$ concentration increases, $T_N(x)$ decreases and the quadratic dependence $\sigma_D(T)$ is rapidly superseded by a linear dependence $\sigma_D(T) \propto (1 - \eta T/T_N)$ in a wide temperature interval (Fig. 2). The function $\sigma_D(T)$ is not perfectly linear for $T < 3$ K, $x = 0.37$ (Fig. 2), but the deviation is very slight; for $x = 0.28$, $\sigma_D(T)$ is linear down to $T = 2$ K.

The magnetic properties of the crystals in the antiferromagnetic state reflect the random distribution of the interacting magnetic moments of the Ni^{++} ions in the $\text{Ni}_{1-x}(\text{Zn, Mg})_x\text{F}_2$ crystal lattice. This distribution should clearly be less uniform than a Gaussian distribution for crystals in which the Ni^{++} ions do not form clusters.

The crystals can be classified in terms of the constant $\Theta(x)$ in the Curie-Weiss law for the magnetic susceptibility. For ions with a Gaussian distribution, the probability for a given ion to have n nearest neighbors at a given concentration x is given by

$$P(n) = \frac{8!}{(8-n)! n!} x^n (1-x)^{8-n}.$$

The constant $\Theta(x)$ is given by

$$\Theta(x) = \sum_i^8 P(n) n \Theta_0,$$

where Θ_0 is the value of Θ for two neighboring magnetic ions. Substituting the expression for $P(n)$ into the formula for $\Theta(x)$, we obtain

$$\Theta(x) = (1-x)\Theta_{\text{NiF}_2},$$

(x is the concentration of the Zn^{++} or Mg^{++} ions). We can gain information about the distribution of the magnetic ions in the crystal by deducing $\Theta(x)$ from the temperature dependence $\chi^{-1}(T)$ of the inverse susceptibility for $T \gg T_N(x)$ and comparing $\Theta(x)$ with the linear dependence obtained above.

Figure 7 shows χ and $\chi^{-1}(T)$ measured in weak and strong fields with H along the [100] binary axis for $x = 0.63$, $T < 75$ K. The value of Θ obtained from the dependence $\chi^{-1}(T) \propto T + \Theta$ for $T \gg T_N$ in this case is found to be $- (47 \pm 5)$ K. For comparison, Fig. 7 also shows $\chi_1^{-1}(T)$ for $T < 75$ K for an NiF_2 single crystal with $\Theta = -140$ K. We see that the strong-field susceptibility χ_1 measured for $\text{Ni}_{1-x}(\text{Zn, Mg})_x\text{F}_2$ is equal to the magnetic susceptibility for NiF_2 . The value obtained for $\Theta(x)$ demonstrates that the distribution of the interacting magnetic Ni^{++} ions in this crystal lattice is indeed nearly Gaussian.

The increase in the magnetic susceptibility measured in weak magnetic fields as $T < T_N(x)$ decreases may be attributed to the presence in the crystals of isolated Ni^{++} ions surrounded solely by Zn^{++} or Mg^{++} ions. Based on the increase in χ in our specimens as $T \rightarrow 0$, we estimate that these ions made up something on the order of 2-3% of the total number of magnetic ions in the crystals. However, this estimate for the number of free magnetic ions could be much too high, because the magnetic fields $H \approx 30$ kOe at which $M(H, T)$ becomes nonlinear are much stronger than required to reverse the magnetic moments of the free Ni^{++}

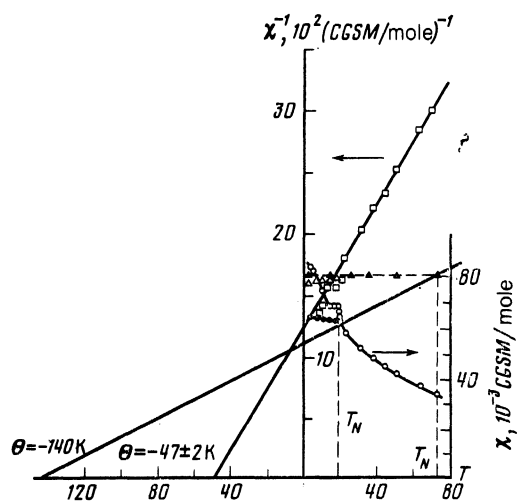


FIG. 7. Temperature dependence of the magnetic susceptibility and its reciprocal for an $\text{Ni}_{0.37}\text{Mg}_{0.63}\text{F}_2$ single crystal measured in weak (< 20 kOe) magnetic fields: \square , $\chi^{-1}(T)$; \circ , $\chi(T)$. The corresponding strong-field dependences are: \bullet , $\chi(T)$ and Δ , $\chi_2^{-1}(T)$. For comparison, \blacktriangle shows the curve $\chi_2^{-1} = \text{const}$ (for $T < T_N$) for an NiF_2 single crystal with $\Theta_{\text{NiF}_2} = -(140 \pm 10)$ K.

ions at the temperature of interest, while the increase in the magnetic susceptibility with $1/T$ measured in weak fields < 20 kOe might also be attributed (as in Refs. 5 and 10, where $Mn_{1-x}Zn_xF_2$ single crystals were studied) to the formation of a magnetic state with a finite correlation radius. Although the shape of the magnetization curves $M(H, T)$ for $Ni_{1-x}(Zn, Mg)_x F_2$ differs markedly from $M(H, T)$ for the $Mn_{1-x}Zn_xF_2$ single crystals¹⁰ at identical nonmagnetic ion concentrations, the increase in χ_1^* and the nonlinearity of $M(H, T)$ in strong fields for the $Ni_{1-x}(Zn, Mg)_x F_2$ single crystals might possibly also be due to the formation of magnetic states with a finite radius.

Figure 8 shows the temperature dependence of the magnetic susceptibilities for $Ni_{0.28}Mg_{0.72}F_2$ measured in magnetic fields $H \approx 4-5$ kOe with $H \parallel [100]$ (curve 1) and $H \parallel [001]$ (curve 2). The susceptibility measured with $H \parallel [001]$ increases with $1/T$ ($T < T_N$) faster than the susceptibility measured with $H \parallel [100]$, possibly due to the formation of a magnetic state with a finite correlation radius. At least two factors can permit such states to form in $Ni_{1-x}(Zn, Mg)_x F_2$: 1) the concentration of the nonmagnetic ions may approach the percolation limit $x_c = 0.76 \pm 0.02$; 2) the effective “ \pm ”-exchange interaction of the magnetic ions is randomly distributed in the plane perpendicular to the tetragonal axis, in which the randomly distributed Dzyaloshinskii interaction also acts. These factors in general cause $\chi_1^*(T)$ to increase with $1/T$ in weak magnetic fields, and it is difficult to distinguish between them under our experimental conditions.

The primary feature of the magnetic properties of the $Ni_{1-x}(Zn, Mg)_x F_2$ single crystals is the fact that the weak ferromagnetic moment $\sigma_D(T)$ starts to depend linearly on temperature as the concentration of the nonmagnetic ions increases (see Figs. 2, 3). A similar temperature dependence of the magnetic moment for dilute antiferromagnets near the percolation limit was found in Ref. 12, where the scaling theory for percolation was used to calculate the state density of the magnetic excitations and also the temperature dependence of the magnetization of the sublattices for an infinite cluster of dilute antiferromagnets.

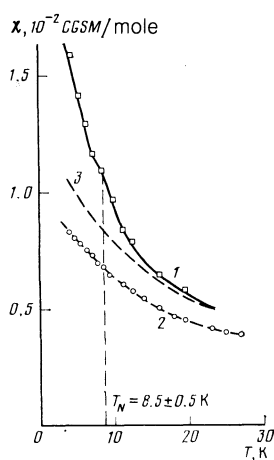


FIG. 8. Magnetic susceptibilities for an $Ni_{0.28}Mg_{0.72}F_2$ single crystal measured in weak magnetic fields, as a function of temperature for $H \parallel [100]$ and $H \parallel [001]$ (curves 1 and 2, respectively). Curve 3 shows the temperature dependence of the magnetic susceptibility measured along the [100] axis and plotted so as to reproduce the observed temperature dependence of the susceptibility measured along the [001] axis.

The linear dependence $M(T)$ obtained in Ref. 12 was found by calculating the magnetization of the system, taking into account the change in the density of states of the magnetic excitations at various temperatures in an infinite cluster when magnetic states (magnetic clusters) with a finite correlation radius are formed. It was found in Ref. 12 that at temperatures $T \ll \omega_0 \ll T_N$ (where ω_0 depends on the correlation radius of the system), the temperature dependence of the magnetic moments of the sublattices obeys the familiar spin-wave law $\Delta M/M \propto T^2$, while for $\omega_0 < T < T_N$ we have $\Delta M/M \propto T$. It was also shown there that the temperature region for which $\Delta M(T)$ is linear is much wider than the spin-wave region. This suggests that magnetic cluster formation at low temperatures is responsible for the linear temperature dependence of the ferromagnetic moment observed in $Ni_{1-x}(Zn, Mg)_x F_2$ as x approaches x_c . States with a finite correlation radius have also been observed to form¹⁻⁴ during cooling of $Mn_{1-x}Zn_xF_2$ and $Co_{1-x}Zn_xF_2$ single crystals with $x \approx x_c$ (in this case directly, by neutron scattering). We did not carry out any neutron scattering experiments on the $Ni_{1-x}(Zn, Mg)_x F_2$ crystals.

Figure 5 shows how the field-dependence of the magnetic moments for the $Ni_{1-x}(Zn, Mg)_x F_2$ single crystals ($x < 0.5$) depends on the orientation ($H \parallel [100]$ or $H \parallel [110]$) as T approaches $T_N(x)$. As in the case of NiF_2 , the vanishing of the orientation dependence for $T \approx T_N(x)$ can be explained by considering the thermodynamic potential Φ (1) which describes the magnetic properties. As in Ref. 6, where the magnetic properties of NiF_2 were studied for $T \approx T_N(x)$, we may neglect the invariants in Eq. (1) of fourth order in M_i , so that the anisotropy disappears. Some relevant experiments and calculations of the direction of the antiferromagnetic vector L for different orientations of H relative to the crystal axes when $T \approx T_N$ are discussed in Ref. 6. All of the conclusions reached there for NiF_2 single crystals extend to the $Ni_{1-x}(Zn, Mg)_x F_2$ crystals we investigated, in which the interacting ions had a near-Gaussian distribution. These values for the effective magnetic fields, which determine the average exchange interaction for the magnetic ions in $Ni_{1-x}(Zn, Mg)_x F_2$, and for their mean anisotropic interactions, which are responsible for the weak ferromagnetism and determine the direction of L , follow from the experimental results presented in Figs. 1 and 2.

In summary, we have shown that as $T < T_N(x)$ decreases, $Ni_{1-x}(Zn, Mg)_x F_2$ single crystals with $x \leq x_c = 0.76 \pm 0.03$ undergo a transition to an antiferromagnetic state with a weak ferromagnetic moment $\sigma_{D\perp}$. The concentration of the nonmagnetic ions greatly influences the transition temperature $T_N(x)$ to the antiferromagnetic state but has little effect on $\sigma_{D\perp}$, the magnetic susceptibility χ_1 , or the effective Dzyaloshinskii interaction H_D in crystals with $x < 0.63$. The magnetic properties of the crystals are distinguished by a nonlinear dependence $M(H, T)$ at higher Zn^{++} or Mg^{++} concentrations when the magnetic field is normal to the tetragonal axis, and by the linear temperature dependence $\sigma_{D\perp}(T)$ of the weak ferromagnetic moment. These features may be ascribed to the low-temperature formation of magnetic states with a finite correlation radius, in which the Ni^{++} magnetic moments are randomly aligned in the (001) plane. These magnetic cluster form in $Ni_{1-x}(Zn, Mg)_x F_2$ with $x \approx x_c$ because the effective “ \pm ”-exchange and anisotropic interactions (including the Dzyaloshinskii

interaction) are randomly distributed.

We are most grateful to A. S. Borovik-Romanov for his unflagging interest in this work and for a discussion of the results.

- ¹M. Hagen, R. A. Cowley, S. K. Satija, *et al.*, Phys. Rev. B **28**, 2602 (1983).
- ²R. J. Birgenau, R. A. Cowley, G. Shirane, and H. Yoshizawa, Phys. Rev. Lett. **54**, 2147 (1985).
- ³D. P. Belanger, A. R. King, and V. Jaccarino, Phys. Rev. B **31**, 4538 (1985).
- ⁴H. Yoshizawa, R. A. Cowley, G. Shirane, and R. Birgenau, Phys. Rev. B **31**, 4548 (1985).
- ⁵A. N. Bazhan and S. V. Petrov, Zh. Eksp. Teor. Fiz. **84**, 315 (1983)

[Sov. Phys. JETP **57**, 181 (1983)].

⁶A. S. Borovik-Romanov, A. N. Bazhan, and N. M. Kreñes, Zh. Eksp. Teor. Fiz. **64**, 1367 (1973) [Sov. Phys. JETP **37**, 695 (1973)].

⁷J. Lockwood, Appl. Phys. **51**, 59 (1982).

⁸A. N. Bazhan, A. S. Borovik-Romanov, and N. M. Kreñes, Prib. Tekh. Eksp., No. 1, 213 (1973).

⁹A. S. Borovik-Romanov and V. I. Ozhogin, Zh. Eksp. Teor. Fiz. **39**, 27.

¹⁰A. N. Bazhan and S. V. Petrov, Zh. Eksp. Teor. Fiz. **86**, 2179 (1984) [Sov. Phys. JETP **59**, 1269 (1984)].

¹¹I. E. Dzyaloshinskii, Zh. Eksp. Teor. Fiz. **33**, 1454 (1957) [Sov. Phys. JETP **6**, 1120 (1958)].

¹²I. Ya. Korenblit and E. F. Shender, Usp. Fiz. Nauk **126**, 233 (1978) [Sov. Phys. Uspekhi **21**, 832 (1978)].

Translated by A. Mason